JOURNAL OF MATERIALS SCIENCE **35** (2000) 5537–5543

# Nanocrystallization of Ge-Al-Cr-Ce-Sm alloy

D. V. LOUZGUINE*, A. TAKEUCHI, A. INOUE
*Institute for Materials Research, Tohoku University, Katahira 2-1-1, Aoba-Ku, Sendai 980-8577, Japan*
*E-mail: dmluz@imrtuns.imr.tohoku.ac.jp*

$Ge_{68}Cr_{14}Al_{10}Ce_4Sm_4$ amorphous alloy was found to have a multistage crystallization behaviour. First stage of crystallization has been studied by differential scanning calorimetry, X-ray diffraction and transmission electron microscopy including high-resolution imaging. This phase transformation can not be described just by one of the following mechanisms: polymorphous, eutectic, primary and spinodal decomposition and is rather a combination of the polymorphous and primary crystallization. An activation energy *E* (an energy barrier opposing a reaction) obtained using Kissinger analysis from the shift of the peak temperature in the DSC curve was 360 kJ/mol. Crystalline structure of an unknown phase formed under heating was studied. 

## 1. Introduction

According to classical point of view four distinct types of phase transformation mechanisms were observed during crystallization of the metallic glasses (metallic amorphous materials) i.e. polymorphous, eutectic, primary and spinodal decomposition [1]. The present paper aims to present a first-stage crystallization reaction of a Ge-Cr-Al-Ce-Sm alloy that could hardly be referred to one of the mechanisms described above. Ge is a semiconductor and a semi-metal. However the $Ge_{68}Cr_{14}Al_{10}Ce_4Sm_4$ alloy studied in the present paper contains 32 at% of metals and can be treated as metallic amorphous material.

Quaternary Ge-Al-Cr-TM amorphous alloys have been obtained and studied recently [2]. It has been noted that, although an amorphous-type X-ray diffraction pattern was observed, the structure of new multicomponent Ge-based alloys in the as-solidified state consisted of extremely small (about 1 nm) crystalline-like zones with a certain degree of medium range order distributed homogeneously in an amorphous matrix. The size and distribution of these zones were slightly sensitive to a cooling rate while it was high enough and no crystalline peaks were observed in the X-ray diffraction pattern.

Moreover, local structure of an amorphous $Ge_{50}Al_{40}Cr_{10}$ alloy has been recently studied by conventional X-ray diffraction, anomalous X-ray scattering and transmission electron microscopy including high-resolution imaging [3]. The study showed the inhomogeneous distribution of the alloying elements in the structure of the $Ge_{50}Al_{40}Cr_{10}$ alloy over a very short range of less than 1 nm. The local structures for Ge on one hand and Al, Cr atoms on the other hand were found to be completely different. The partial coordination number in Ge-Ge pair of 3.4 is close to that value of 4 for amorphous Ge. On the other hand the values for other pairs of about 8–10 are closer to that of usual metallic glasses.

## 2. Experimental

An ingot of the $Ge_{68}Cr_{14}Al_{10}Ce_4Sm_4$ alloy was prepared by arc melting the mixture of pure Ge (99.9999 mass%), Al (99.99 mass%) Cr (99.9 mass%) Ce (99.9 mass%) and Sm (99.9 mass%) in an argon atmosphere. The amorphous ribbon samples of about 15 $\mu$m in thickness and 0.9 mm in width were prepared by rapid solidification of the melt on a single copper roller at the roller surface velocity of 42 m/s. The structure of ribbon samples was examined by X-ray diffraction (XRD) with monochromatic Cu $K_\alpha$ radiation and transmission electron microscopy (TEM). TEM was carried out in a JEM 2010 microscope operating at 200 kV equipped with energy dispersive X-ray spectrometer (EDX). Samples for TEM were polished electrolytically in a solution of 10 vol% perchloric acid and 90 vol% methanol at 208–213 K. Crystallization temperature and heat of crystallization were measured by differential isothermal and scanning calorimetry (DSC) at different heating rates.

## 3. Results

After rapid solidification the $Ge_{68}Cr_{14}Al_{10}Ce_4Sm_4$ alloy had an amorphous structure (Fig. 1a). (All figures correspond to $Ge_{68}Cr_{14}Al_{10}Ce_4Sm_4$ alloy if different composition is not indicated). However, as well as in the case of quaternary Ge-Al-Cr-RE alloys finely dispersed zones with elevated medium range order homogeneously distributed in the amorphous matrix were observed using TEM (see Fig. 2 (marked by circles)). Being metastable as-rapidly solidified $Ge_{68}Cr_{14}Al_{10}Ce_4Sm_4$ alloy undergoes phase transformations on heating. Three clearly separated heat effects

* Can be also written as Luzgin.

marked as A, B, and C are observed in the DSC curve taken at a heating rate of 0.667 K/s (Fig. 3). A weak fourth one appeared at the heating rate less than 0.667 K/s is marked as D. Heat released during these transformations at different heating rates is summarised in Table I.

TABLE I Exothermic heat effects on heating

| | Heat effect ($\Delta H$), J/g | | | | |
|---|---|---|---|---|---|
| Heating rate K/s | A | B | C | D | Total (B + C + D) |
| 0.083 | 19.8 | 45.2 | 18.1 | 4.9 | 68.2 |
| 0.167 | 21.8 | 42.4 | 26.8* | | 69.2 |
| 0.333 | 21.2 | 38.3 | 33.6* | | 71.9 |
| 0.667 | 19.7 | 33.9 | 35.9 | — | 69.8 |

*at 0.167 and 0.333 K/s total $\Delta H$ of C and D effects is given.

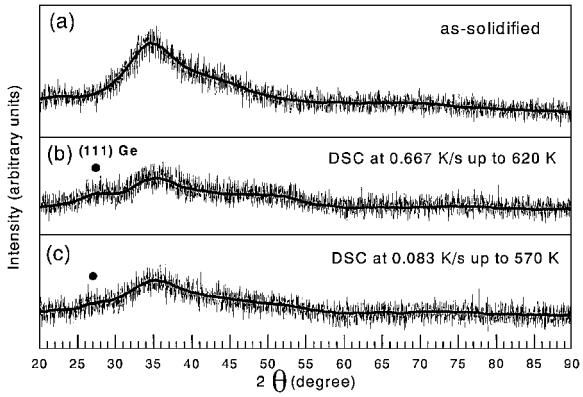


*Figure 1* XRD patterns of the $Ge_{68}Cr_{14}Al_{10}Ce_4Sm_4$ alloy (a) in as-solidified state, (b) after DSC at 0.667 K/s up to 620 K and (c) after DSC at 0.083 K/s up to 570 K.

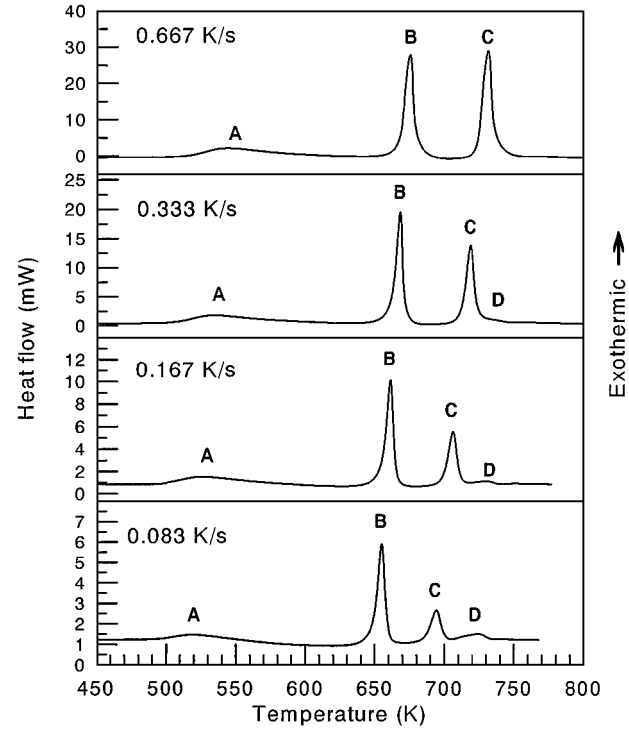


*Figure 3* DSC curves taken at different heating rates.

First prolonged heat effect A is related to the process of structural relaxation of the amorphous matrix. This effect has been studied recently for quaternary $Ge_{70}Cr_{16}Al_{10}Nd_4$ alloy [4]. As can be seen in Fig. 3 this heat effect has not a regular form and consists of at least two heat effects as has been described in Ref. [4]. According to Ref. [4] the major income to this effect has been done by the process of changing of a degree

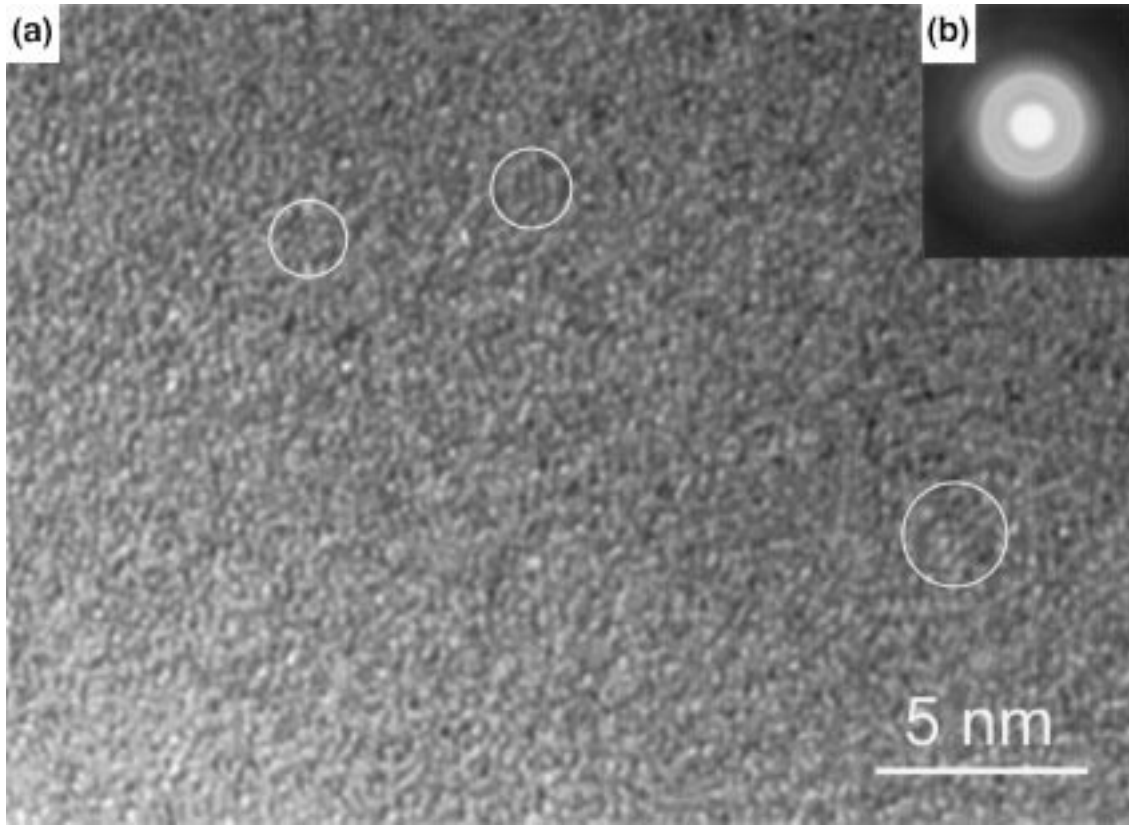


*Figure 2* (a) High-resolution TEM image and (b) selected-area electron diffraction pattern taken in as-solidified state.

of short range order and the formation of tetrahedral configuration of Ge atoms similar to pure a-Ge and c-Ge, arising from the segregation of Ge atoms forming Ge-enriched zones prior to crystallization. The size of such zones is not more than 1 nm. Similar changes of the XRD pattern were observed in the case of the $Ge_{68}Cr_{14}Al_{10}Ce_4Sm_4$ alloy (see Fig. 1) when the first reaction marked as A in Fig. 3 is almost finished but the reaction B has not been started yet. A very broad diffraction peak corresponding to (111) Ge is seen in Fig. 1 (b and c). The breadth of the peak is close to that produced by the amorphous phase suggesting Ge-enriched zones size of less than 1 nm. It reflects the same process of formation of tetrahedral configuration of Ge atoms similar to pure a-Ge that was observed in the $Ge_{70}Cr_{16}Al_{10}Nd_4$ alloy. No crystalline phase(s) were observed at this stage using TEM.

Type of the reaction B is the main purpose of study in the present work. As the onset temperature of the reaction C is quite close to B it is hard to control the temperature and time of isothermal annealing in furnace. However, DSC gives a great opportunity to observe passing of the reaction through a heat released and to stop heating exactly at the desired temperature. Cooling rate of the tested specimen was about 0.6–0.7 K/s for the first 100 K. Ribbon specimens cut to pieces were heated up to the completion of the reaction B at different heating rates of 0.083, 0.167, 0.333 and 0.667 K/s. Heating has been stopped at 660, 667, 673 and 683 K respectively. Temperature difference from the onset point of the reaction C in every case was more than 20 K, that is enough to have no influence of this subsequent reaction. XRD patterns corresponding to the above-mentioned samples are shown in Fig. 4. Three broadened diffraction peaks belong to pure Fd3m Ge. As shown in Fig. 5 the structure of the sample heat treated at 0.667 K/s consists of the equiaxed nanoscale Ge particles with the size of about 3–20 nm homogeneously distributed in the amorphous matrix. With the reduction of the heating rate an unknown crystalline phase started to nucleate and grow simultaneously (see Fig. 4). Very weak crystalline peaks belonging to this phase are also seen in the XRD pattern of the samples heat treated at 0.667 K/s. As can bee seen from Fig. 5c three sharp diffraction rings in selected-area electron diffraction (SAED) pattern belong to Fd3m Ge. However, some strong dot-like reflections are seen between these rings. A quite large particle marked be arrow is seen in Fig. 5a. This particle is not seen in the dark-field image (Fig. 5b) taken from the first ring corresponding to (111) Ge of SAED pattern (Fig. 5c). Being also larger than the Ge particles this particle likely belongs to the unknown crystalline phase.

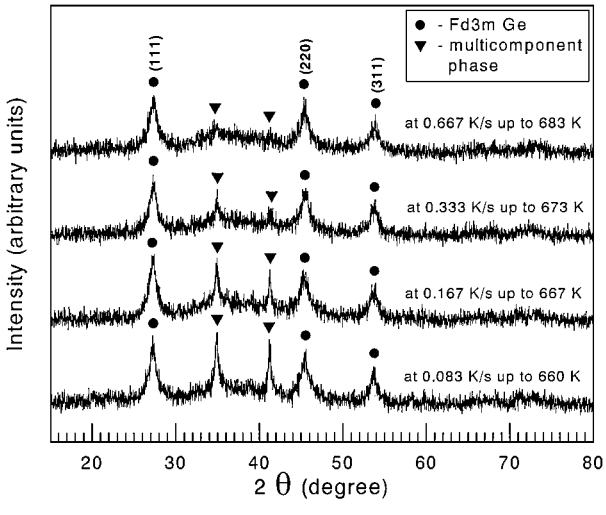


*Figure 4* XRD patterns of the samples heat treated using DSC carried out at the heating rates of 0.083, 0.167, 0.333 and 0.667 K/s up to 660, 667, 673 and 683 K respectively.

Average Ge particles size was calculated from the broadening of the diffraction peaks. The X-ray powder diffraction pattern of pure Ge was used as a reference. Intrinsic broadening of the diffraction peak $\beta$ for the cubic lattice can be calculated by the following Equation [5]

$$\beta = 0.5B\left(1 - \frac{b}{B} + \sqrt{1 - \frac{b}{B}}\right), \tag{1}$$

where $b$ is instrumental broadening and $B$ is total line broadening of the diffraction peak. A part of the intrinsic broadening of the diffraction peak caused by small particles size effect $m$ can be separated from the part of broadening caused by microdeformation $n$ by the following formulas [5]:

$$\frac{m_1}{\beta_1} = \frac{1}{2}\left(1 - 4\frac{n_1}{\beta_1} + \sqrt{8\frac{n_1}{\beta_1^2} + 1}\right) \tag{2}$$

$$\frac{\beta_2}{\beta_1} = \frac{\left(\frac{1}{2}V\frac{m_1}{\beta_1} + 2\frac{n_1}{\beta_1}W\right)^2}{\frac{1}{2}V\frac{m_1}{\beta_1} + 4\frac{n_1}{\beta_1}W} \tag{3}$$

$$V = \frac{m_1}{m_2} = \frac{\cos\theta_1}{\cos\theta_2} \tag{4}$$

$$W = \frac{n_2}{n_1} = \frac{\mathrm{tg}\theta_2}{\mathrm{tg}\theta_1} \tag{5}$$

The average particle size $D_{hkl}$ in the direction normal to the ($hkl$) plane can be calculated from Equation 6

$$D_{hkl} = \frac{0.94\lambda}{m_1\ \cos\theta_1} \tag{6}$$

where $\lambda$ is wavelength (nm) and $\theta$ is the diffraction angle (rad). The resulted $D$ size of 11.3 nm is in good agreement with TEM observations (see Fig. 5). According to TEM results Ge particles size ranges from 3 to 20 nm (see Fig. 5).

According to the XRD data (see Fig. 4) the Fd3m Ge particles size is independent of the heating rate whereas the size and volume fraction of the unknown phase are strongly heating rate dependent that effects on the half width and height of the corresponding crystalline peaks (see Figs 4 and 5). The unknown crystalline phase of dendritic morphology formed after heat treatment using DSC at 0.083 K/s attained several hundreds of nanometers in size (Fig. 6). Fig. 7a–d shows diffraction patterns

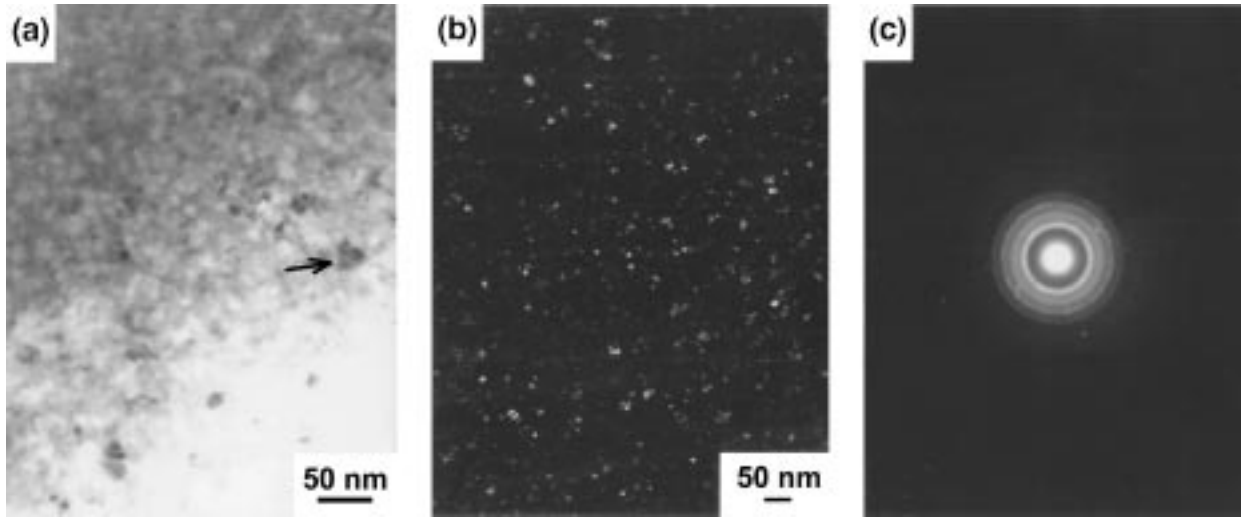


*Figure 5* Nanoscale crystalline precipitations in the amorphous matrix. (a) Bright-field, (b) dark-field image and (c) selected area electron diffraction pattern taken from a group of particles including residual amorphous matrix. A sample heat treated using DSC at 0.667 K/s up to 683 K.

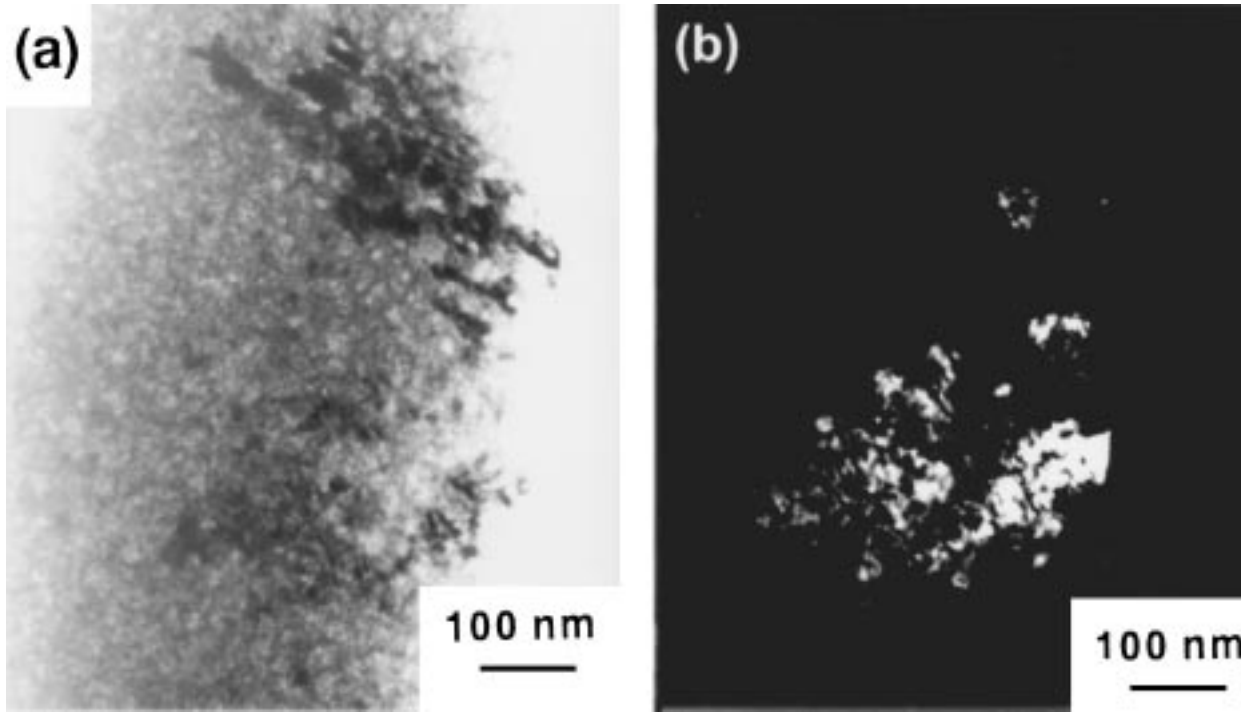


*Figure 6* Particles of the multicomponent $Ge_{18}Cr_4AlCeSm$ phase in the sample heat treated using DSC at 0.083 K/s up to 660 K. (a) Bright-field and (b) dark-field images.

taken from the multicomponent crystalline phase. It is important to note that a significant volume fraction of the residual amorphous matrix still existed in the structure after the completion of the reaction B.

The unknown crystalline phase is a multicomponent one. It contains in average 71.5 at% Ge, 16.6 at% Cr, 4 at% Al, 4 at% Ce and 3.9 at% Sm and can be written as $Ge_{18}Cr_4AlCeSm$. Except for low Al content, chemical composition of this phase is very close to the composition of the as-solidified amorphous matrix. This multicomponent phase is a metastable one and disappeared during reactions C and D. Ge particles grew and those XRD peaks became narrower. After the complete of all phase transformations the structure consists of Fd3m Ge and another unknown phase(s) (Fig. 8 after DSC up to 768 K).

## 4. Discussion

According to Table I and Fig. 3 redistribution of the values of heat effects B, C and D on DSC curves takes place under changes of a heating rate. Value of the effect B increases in expense of the effects C and D. However, it is important to note that through the volume fraction of the multicomponent phase and heat effect of the B-exothermic reaction change with the heating rate the shape of the B-curve in all cases suggests passing of a single phase transformation. More clearly it can be seen in Fig. 9 that shows differential calorimetry measurements of the reaction B in isothermal mode at 630 K. B-curve has a regular form that is usual for a single-stage transformation. XRD pattern of the sample heat treated for 2.7 ks in isothermal mode at 630 K is similar to that one taken after DSC at 0.083 K/s up to 660 K (see

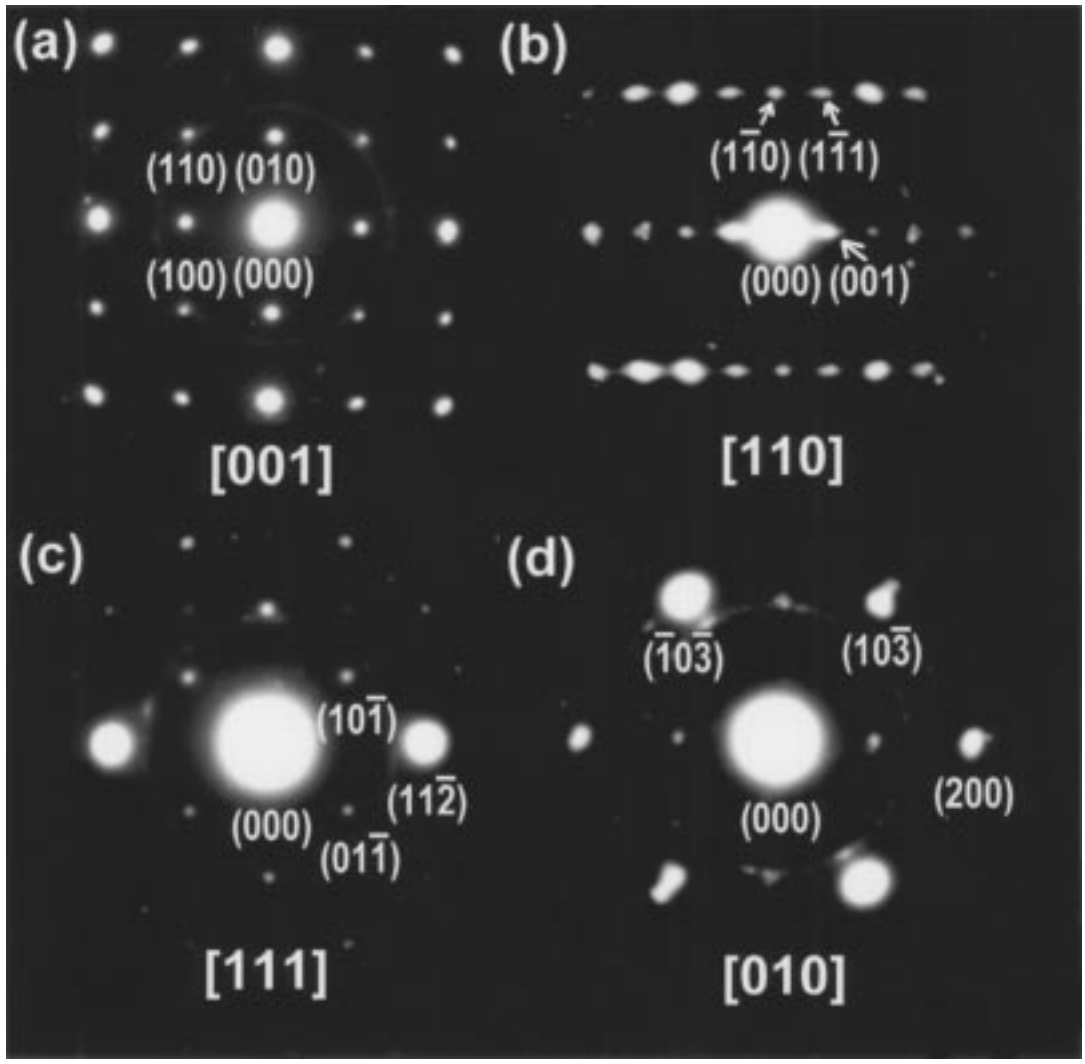


*Figure 7* (a–d) Selected area electron diffraction patterns taken from the crystalline particles of the multicomponent $Ge_{18}Cr_4AlCeSm$ phase (Fig. 6) (zone axes [001], [110], [111] and [010] and those indexing. Sharp rings belong to (111) Ge.

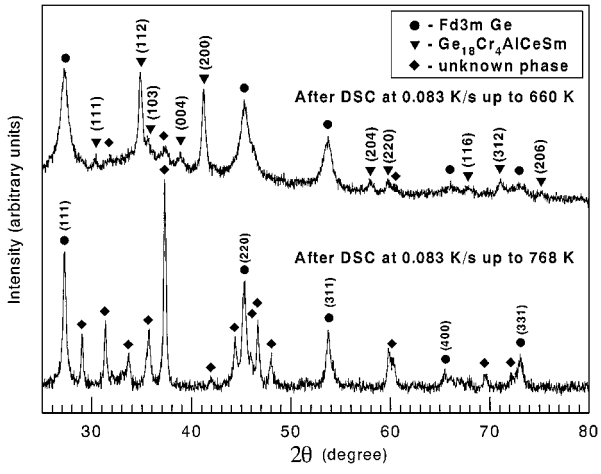


*Figure 8* XRD patterns of the samples heat treated using DSC at a heating rate of 0.083 K/s up to 660 and 768 K respectively.

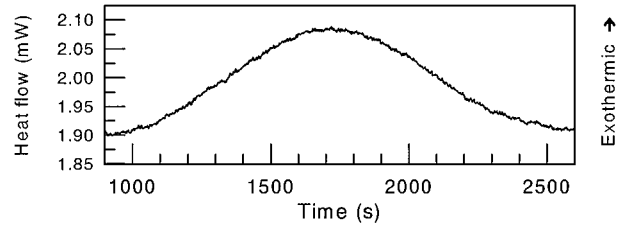


*Figure 9* Isothermal differential calorimetry curve taken at 630 K.

Fig. 4). Kinetic studies conducted at 630 K showed that XRD peaks belonging to Fd3m Ge and multicomponent phase appear and intensify simultaneously during phase transformation in isothermal mode.

Thus, precipitation of Ge nanoparticles as well as nucleation and growth of the multicomponent phase go simultaneously. As an example of the opposite case one can show DSC curve of the quaternary $Ge_{70}Cr_{16}Al_{10}Nd_4$ alloy in which two different crystallization reactions are close to each other on temperature (follow arrows in Fig. 10). These two heat effects became more clearly separated as the heating rate decreases.

The largest part of the reaction B is caused by formation of the Ge particles as precipitation of the multicomponent phase (see Table I) gives a lower income to the total heat effect. It can be suggested that the Ge nanoparticles grew from the Ge – enriched zones formed during structural relaxation. As chemical composition of the $Ge_{18}Cr_4AlCeSm$ multicomponent phase

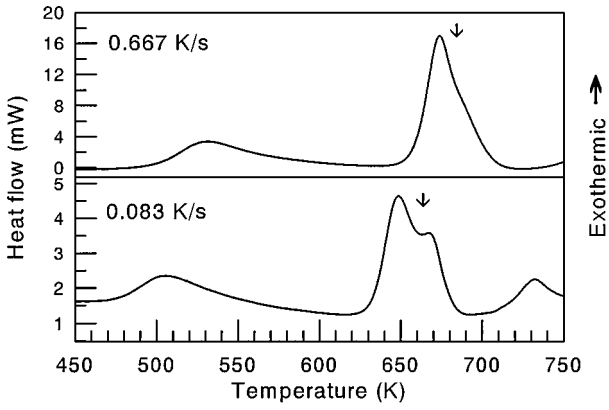


*Figure 10* DSC curves of $Ge_{70}Cr_{16}Al_{10}Nd_4$ alloy taken at two different heating rates.

TABLE II Experimental and calculated $d$-spacings and experimental relative integrated intensities for the $Ge_{18}Cr_4AlCeSm$ metastable phase having a tetragonal lattice of $a = 0.438$ nm and $c = 0.925$ nm

| $d$-spacings, nm | | Relative integrated | |
|---|---|---|---|
| experimental | calculated | Intensities, $I/I_0$ | *HKL* |
| 0.2939 | 0.2937 | 5 | (111) |
| 0.2573 | 0.2573 | 100 | (112) |
| 0.2520 | 0.2521 | 11 | (103) |
| 0.2315 | 0.2313 | 9 | (004) |
| 0.2190 | 0.2190 | 95 | (200) |
| 0.1590 | 0.1590 | 12 | (204) |
| 0.1546 | 0.1547 | 14 | (220) |
| 0.1380 | 0.1380 | 7 | (116) |
| 0.1326 | 0.1327 | 15 | (312) |
| 0.1261 | 0.1261 | 4 | (206) |

TABLE III Experimental and calculated $d$-spacings and angles between some crystallographic planes in a tetragonal lattice of $a = 0.438$ nm and $c = 0.925$ nm according to selected-area diffraction patterns of Fig. 7

| Zone axis | Plane 1 | Plane 2 | Angle between two planes, degree | |
|---|---|---|---|---|
| *uvw* | $h_1k_1l_1$ | $h_2k_2l_2$ | Experimental | Calculated |
| [001] | (100) | (110) | 45 | 45 |
| | (100) | (010) | 90 | 90 |
| | (110) | (010) | 45 | 45 |
| [110] | (1 − 10) | (1 − 11) | 19 | 18.5 |
| | (1 − 10) | (001) | 90 | 90 |
| | (1 − 11) | (001) | 71 | 71.5 |
| [111] | (10 − 1) | (11 − 2) | 40 | 39.7 |
| | (10 − 1) | (01 − 1) | 80 | 79.4 |
| | (01 − 1) | (11 − 2) | 40 | 39.7 |
| [010] | (−10 − 3) | (10 − 3) | 70 | 70.2 |
| | (−10 − 3) | (200) | 124 | 125.1 |
| | (10 − 3) | (200) | 54 | 54.9 |

is close to composition of the amorphous matrix it likely nucleates by polymorphous mechanism. The Ge nanoparticles precipitate homogeneously in the amorphous matrix (see Fig. 5) and often have no common interface with multicomponent phase (Figs 5 and 6) i.e. Ge particles are located in the residual amorphous matrix between large particles of multicomponent phase. In Fig. 6 Ge particles embedded in amorphous matrix are seen in the bright-field image and not seen in the dark-field one taken in the reflection produced by the multicomponent phase. Both Fd3m Ge and multicomponent phase are homogeneously distributed in amorphous matrix, but the distance between particles of the multicomponent phase is about several $\mu$m whereas the distance between the Ge particles is much lower being several tens of nm. Thus, although formation of these two phases takes place simultaneously no eutectic-type coupled growth was observed.

At any heating rate in the range from 0.083 to 0.667 K/s temperature difference between onset temperature of the reaction B and its offset temperature is about 20 K. Considering difference in the heating rate one can calculate a reaction time. At the heating rates of 0.083, 0.167, 0.333 and 0.667 K/s, with the corresponding temperature difference of 23, 21, 19 and 22 K, respectively, B-reaction lasted for 276, 126, 57 and 33 seconds, respectively. Such a time difference is a reason for the large-size multicomponent particles observed in the samples heat treated at 0.083 K/s and those high volume fraction.

Multicomponent $Ge_{18}Cr_4AlCeSm$ phase was found to have a tetragonal lattice of $a = 0.438$ nm and $c = 0.925$ nm. In order to distinguish X-ray diffraction peaks of low intensity XRD of the sample heat treated up to the completion of the reaction B has been done in a step scan mode (see Fig. 8 DSC up to 660 K). Experimental and calculated $d$-spacings for the $Ge_{18}Cr_4AlCeSm$ phase given in Table II were found to be in a good agreement. Tetragonal structure has been proposed on the basis of the diffraction patterns shown in Fig. 7a–d. Those indexing is done according to the lattice proposed. Zone axis of every section of the reciprocal lattice is given below the picture in square brackets. Radius of the (111) Ge ring has been used as a reference for the determination of the diffraction constant $\lambda L$ - product of the electron wavelength and the distance of the specimen from the screen. In some of patterns (Fig. 7) such a ring is hardly visible due to increase of contrast during printing. However, such a ring is clearly seen in all original negative images used for analysis. Experimental and calculated angles between crystallographic planes according to the sections [001], [110], [111] and [010] of reciprocal lattice (Fig. 7), respectively, are summarized in Table III.

Multicomponent $Ge_{18}Cr_4AlCeSm$ phase being metastable disappears on subsequent heating and another unknown phase(s) forms (Fig. 8). Analysis of the structure of this phase(s) is out of the purpose of this paper. It can be a multicomponent phase or one of two phases with unknown structure observed in ternary Ge-Al-Cr system [6].

Metallic amorphous alloys quite often have so called as-quenched nuclei of crystalline phase or medium range order zones that use to be the centres of the subsequent crystallization [7]. However, crystallization of such a glass follows one of the four mechanisms described in the introductory part. In the present Ge-based amorphous alloy two different phases often having no common interface (that should exist in the case of eutectic reaction or spinodal decomposition) grew simultaneously from the amorphous matrix.

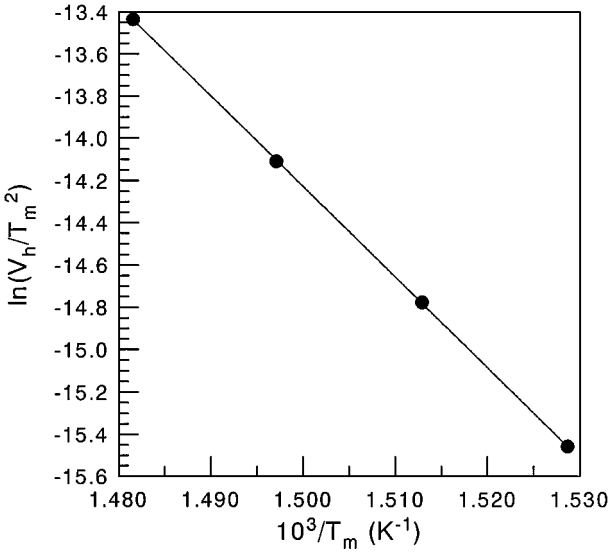


*Figure 11* Kissinger plot.

An activation energy $E$ (the energy barrier opposing the reaction B) was obtained using Kissinger analysis [8] from the shift of the peak temperature in the DSC curve ($T_m$) using equation:

$$-\frac{E}{R} = \frac{d\left(\ln V_h / T_m^2\right)}{d(1/T_m)} \quad (7)$$

Kissinger plot ($\ln V_h / T_m^2$) vs. ($1/T_m$) is shown in Fig. 11. The calculated activation energy is 360 kJ/mol. Linear shape of the Kissinger plot suggests no change of the transformation mechanism at different heating rates.

## 5. Conclusions

$Ge_{68}Cr_{14}Al_{10}Ce_4Sm_4$ amorphous alloy has a multistage crystallization process. After the completion of the structural relaxation process on the first stage of crystallization two crystalline phases: Fd3m Ge and the multicomponent $Ge_{18}Cr_4AlCeSm$ phase nucleate and grow simultaneously during a single stage transformation. The size and volume fraction of the multicomponent phase depends upon the heating rate used whereas the size and distribution of the Ge particles are independent of the heating rate. Such a phase transformation can not be described by one of the following mechanisms: polymorphous, eutectic, primary and spinodal decomposition. It looks like a combination of the polymorphous and primary crystallization. Multicomponent $Ge_{18}Cr_4AlCeSm$ phase is a metastable phase and disappears during subsequent heating. This phase was found to have a tetragonal lattice of $a = 0.438$ nm and $c = 0.925$ nm. It can be suggested that Ge nanoparticles grew from the Ge – enriched zones formed during structural relaxation. As chemical composition of the multicomponent phase is close to composition of the amorphous matrix it likely nucleates by polymorphous mechanism.

## Acknowledgements

This work was partially supported by a Grant-in-Aid for Scientific Research from the Ministry of Education, Science and Culture of Japan (N: 11750634).

## References

1. R. W. CAHN, in "Physical Metallurgy," edited by R. W. Cahn and P. Haasen (North-Holland Elsevier Publishers, 1983) p. 1827
2. D. V. LOUZGUINE and A. INOUE, *Mater. Trans., JIM* **40** (1999) 485.
3. D. V. LOUZGUINE, M. SAITO, Y. WASEDA and A. INOUE, *J. Phys. Soc. Jap.* **68** (1999) 2298.
4. D. V. LOUZGUINE, A. INOUE, M. SAITO and Y. WASEDA, *Scr. Mater.* **42** (2000) 289.
5. S. S. GORELIK, U. A. SKAKOV and L. N. RASTORGUEV, "X-ray and Electron-optic Analysis" (Moscow, MISIS, 1994) p. 137 (in Russian).
6. V. V. MILYAN and YU. B. KUZ'MA, *Russian Metallurgy* (translated from Izvestia Akademii Nauk SSSR, Metally) **4** (1987) 191.
7. A. L. GREER, *Mater. Sci. Eng.* **A179/180** (1994) 41.
8. H. E. KISSINGER, *J. Res. National. Bureau Stand.* **57** (1956) 217.

*Received 22 November 1999*
*and accepted 8 May 2000*